

Analysis of the packaging enclosing a counterfeit pharmaceutical tablet using Raman microscopy and two-dimensional correlation spectroscopy

Kaho Kwok, Lynne S. Taylor*

Department of Industrial and Physical Pharmacy, College of Pharmacy, Purdue University, 575 Stadium Mall Drive, West Lafayette, IN 47907, USA

ARTICLE INFO

Article history:

Received 30 November 2011
 Received in revised form 24 February 2012
 Accepted 28 February 2012
 Available online 7 March 2012

Keywords:

Counterfeit
 Raman
 Two-dimensional correlation spectroscopy
 Packaging
 Pharmaceutical

ABSTRACT

Counterfeit medicine is a serious global problem. Vibrational spectroscopy combined with chemometric methods can be used to combat the pharmaceutical counterfeit problem. In this study, packages containing counterfeit tablets were analyzed using Raman microscopy and two-dimensional correlation spectroscopy. Two color regions were analyzed and different chemical origins from the color region could be resolved by two-dimensional correlation spectroscopy. Univariate Raman images were used to show the spatial distribution of the chemical components and confirm the findings of two-dimensional correlation analysis.

© 2012 Elsevier B.V. All rights reserved.

1. Introduction

Approximately 10% of the available pharmaceuticals worldwide are thought to be counterfeits; however this number is likely to be an underestimation due to the difficulty in monitoring the problem [1]. Counterfeit medicines not only occur in the developing countries, but are also becoming increasingly prevalent in developed countries due to the widespread use of lower cost, but poorly regulated, internet pharmacies. For example, counterfeit over-the-counter weight-loss medicine Alli® pills were obtained from an Internet supplier in 2010 [2]. These counterfeit Alli® pills contained an active pharmaceutical ingredient (API) called sibutramine instead of orlistat which is present in authentic Alli® pills. In 2009, a counterfeit diabetic medicine containing six times the normal dose of the blood sugar lowering agent glibenclamide was discovered in China [3]. These counterfeit diabetic drugs caused two deaths and nine hospitalizations. Counterfeit schizophrenia medicine Zyprexa® was discovered in the United Kingdom supply chain in 2007 [4]. The counterfeits contained only 60% of the labeled amount of API. These are just a few recent examples of the widespread pharmaceutical counterfeit problem.

The World Health Organization (WHO) defines counterfeit medicine as medicines that are deliberately and fraudulently mislabeled with respect to identity and/or source [5]. As the sophistication and prevalence of counterfeit pharmaceuticals escalates, it

becomes increasingly important to develop analytical approaches to differentiate between genuine and fake products.

Two-dimensional correlation spectroscopy (2dcos) has been used to solve numerous spectroscopic problems. It was introduced and developed in the 1980s by Noda [6]. A brief description of 2dcos will be given here; interested readers can consult the literature for a more detailed theoretical description [6–9]. 2dcos is a data analysis technique that can convert a series of one-dimensional spectra into two-dimensional maps. The basic concept is to introduce an external perturbation into the system under study to generate dynamic spectra. The dynamic spectra are subject to correlation analysis to generate a two-dimensional synchronous and an asynchronous map. The synchronous map displays the similarities in intensity changes, while the asynchronous map displays the dissimilarities in spectral variations. The following equations show the matrix representation of synchronous and asynchronous maps. For the synchronous map:

$$\Phi(\nu_1, \nu_2) = \frac{1}{m-1} \sum_{j=1}^m \tilde{y}_j(\nu_1) \cdot \tilde{y}_j(\nu_2) \quad (1)$$

where ν are the wavenumbers, m is the number of samples, and \tilde{y} are the dynamic spectra [8].

For the asynchronous map:

$$\Psi(\nu_1, \nu_2) = \frac{1}{m-1} \sum_{j=1}^m \tilde{y}_j(\nu_1) \cdot \tilde{z}_j(\nu_2) \quad (2)$$

* Corresponding author. Tel.: +1 765 496 6614; fax: +1 765 494 6545.
 E-mail address: lstaylor@purdue.edu (L.S. Taylor).



Fig. 1. Photographs of Cialis® packages (left: genuine; right: counterfeit). (For interpretation of the references to color in the text, the reader is referred to the web version of the article.)

where z is the transformation of y :

$$\tilde{z}_j(\nu_2) = \sum_{k=1}^m N_{jk} \cdot \tilde{y}_k(\nu_2) \quad (3)$$

and N is the Noda–Hilbert transformation matrix, where $N_{jk} = 0$ if $j = k$, otherwise $N_{jk} = 1/[\pi(k - j)]$ [8].

Raman spectroscopy is a powerful diagnostic and analytical tool and has been utilized broadly for pharmaceutical applications [10–15]. Raman spectroscopy can be combined with microscopy to analyze microscopic chemical features of a sample. One of the main advantages of this combination is that a two dimensional chemical image or map can be generated to provide detailed chemical information of the surface. Raman microscopy has been used to analyze a broad range of samples, including pharmaceuticals [16,17]. Recently, researchers have shown that it is possible to combine Raman microscopy with 2dcos to analyze pharmaceutical tablets where the researchers used the vertical image coordinate as the perturbation of the system to generate the dynamic spectra [18].

The objective of the current study was to combine Raman microscopy and 2dcos for the analysis of counterfeit packaging, using the vertical image coordinate as the perturbation of the system to generate the dynamic spectra. Being able to detect and analyze the characteristics of the counterfeit packaging could be highly beneficial because it provides an additional dimension to determine the origin of counterfeit medicines. To date, counterfeit drug detection and analysis efforts have focused on subjecting the actual tablet or capsule to chemical and physical analysis. However, the packaging should also be brought to the attention of the researchers since the composition of the packaging such as the colorants and the package material can be as unique as the drug product itself. Colorant analyses using Raman spectroscopy have been performed extensively in the detection of forgeries in fine arts and antiques [19–22]. However, to the best of our knowledge, this type of analysis has not been performed on the packaging of counterfeit medicines. The specific aims of this research include: (1) to analyze the packaging material used for a counterfeit drug product using Raman imaging and two-dimensional correlation

spectroscopy; (2) to evaluate the capability of Raman imaging and 2dcos in analyzing colorant components on counterfeit packages.

2. Materials and methods

2.1. Materials

The external carton packaging used to hold blister packs of tablets of the erectile dysfunction drug Cialis® was analyzed in this work. Cialis® tablets in this type of packaging are sold in Europe while in the United States they are packaged in plastic bottles. Therefore, the genuine Cialis® package was obtained legally through a pharmacy in Turkey. The counterfeit Cialis® package was obtained from Eli Lilly and Company (Indianapolis, IN). Microcrystalline cellulose (MCC) was obtained from FMC Corporation (Philadelphia, PA) and calcium carbonate was obtained from Alfa Aesar (Ward Hill, MA).

2.2. Methods

Two (white and yellow) color regions were chosen for the analysis (Fig. 1).

Raman microscopy was performed using a Renishaw model 1000 Raman microscope (Gloucestershire, UK). The laser wavelength was 783 nm and the laser power was 23–26 mW. The magnification of the objective was 50× (0.75 N.A.) (Leica, Buffalo Grove, IL). The wavenumber accuracy of the spectrograph was about 1–2 cm^{-1} . The spectral range collected was from approximately 950 to 1500 cm^{-1} or 1150 to 1650 cm^{-1} depending on the color region. The sampling area was 400 $\mu\text{m} \times 400 \mu\text{m}$ and the step size was 20 μm , this yields to a total of 441 spectra for a single correlation map. Spectra were collected using the mapping mode of the WiRE software (Version 1.3, Renishaw). Spectra were subject to pre-processing before being analyzed by the 2dcos method. Data pre-processing includes the following: (1) normalization of the spectra based on the mean of each spectrum; (2) cosmic ray removal using the algorithm by Cappel et al. [23]; (3) baseline correction using the algorithm by Lieber et al. [24]; (3) spectral smoothing using the Savitzky–Golay algorithm [25]; and

(4) spectral truncation to remove erratic features at either end of the spectral region due to baseline correction and smoothing procedures.

The vertical image coordinate was used as the perturbation in the 2dcos analysis [18]. Both average and zero spectra were examined for use as the reference spectrum in the 2dcos analysis. For synchronous spectra, the average spectrum was used as the reference spectrum to calculate the dynamic spectra because the zero spectrum only produced positive cross peaks in the synchronous map since the synchronous map generated this way is only the cross product of the two data matrices with no negative components. However, the zero spectrum was used as the reference spectrum to calculate the dynamic spectra for the asynchronous maps. Early analyses showed that cross peaks occurred at spectral positions that cannot be found in the original spectra if the average spectrum was used as the reference spectrum; therefore the zero spectrum was used as the reference spectrum.

All data analyses and graphing were performed using programs and built-in codes written in the MATLAB language (Mathworks, Natick, MA).

3. Results and discussion

The photographs of the Cialis® packages are shown in Fig. 1. Both boxes consist of mainly yellow, green and white colors. Although there are a few obvious visual differences between these two boxes, the main purpose of this research is to chemically analyze the box colorants.

3.1. White color region

The set of Raman spectra for the genuine package is shown in Fig. 2a. Visual inspection cannot reveal any correlation of the variations in these spectra. Correlations should become clear with the aid of synchronous and asynchronous maps. The synchronous map of the white color region of the genuine package is shown in Fig. 3. For the synchronous map, there is only one autopeak at 1087 cm^{-1} .

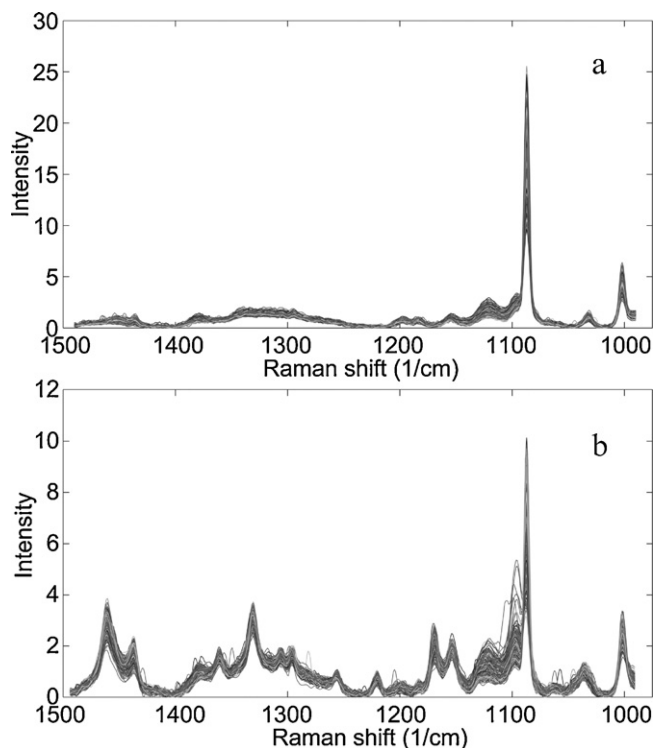


Fig. 2. Raman spectra of the white color region (a: genuine; b: counterfeit).

Autopeaks occur when there is a strong intensity variation at the particular wavenumber. This peak is thought to arise from calcium carbonate which has a strong peak at this wavenumber position (Figs. 4 and 5). Calcium carbonate is commonly used as a white colorant and is also sometimes added as a filler in paper [26]. The fact that there is an autopeak at this wavenumber indicates that the concentration of this compound varies as a function of

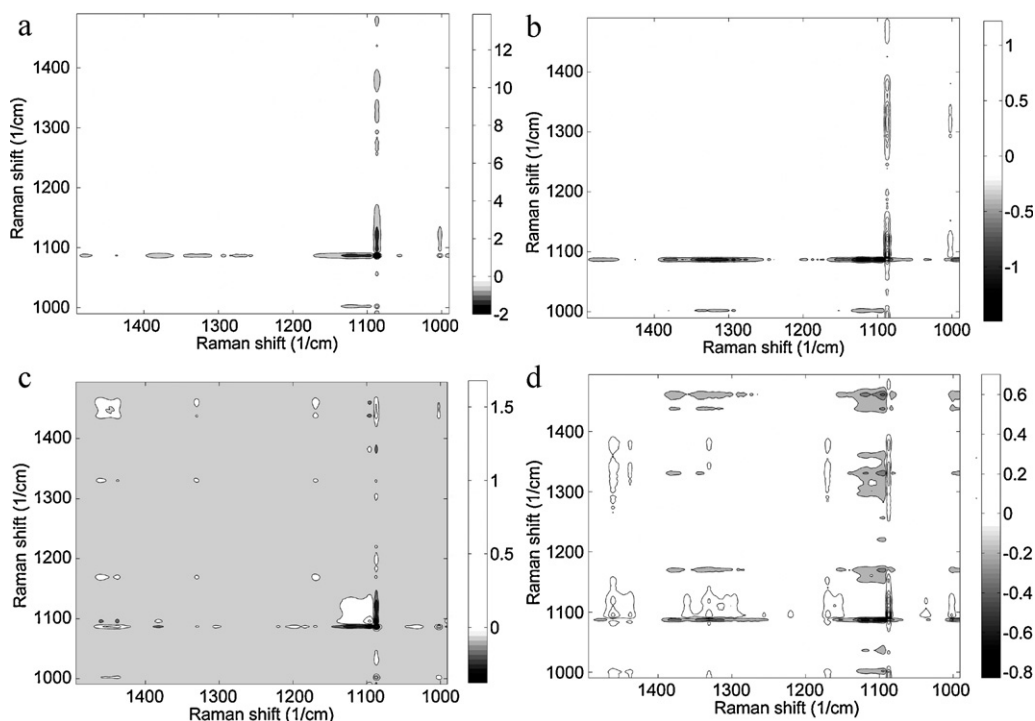


Fig. 3. Synchronous (a and c) and asynchronous (b and d) maps of white color region (a and b: genuine; c and d: counterfeit).

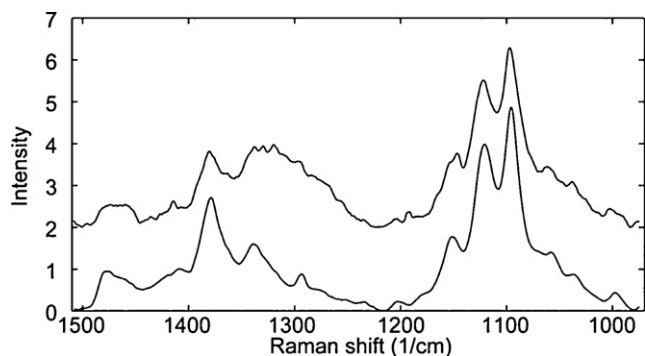


Fig. 4. Raman spectrum of microcrystalline cellulose (bottom) and genuine package box material (inside of box where there is no color) (top).

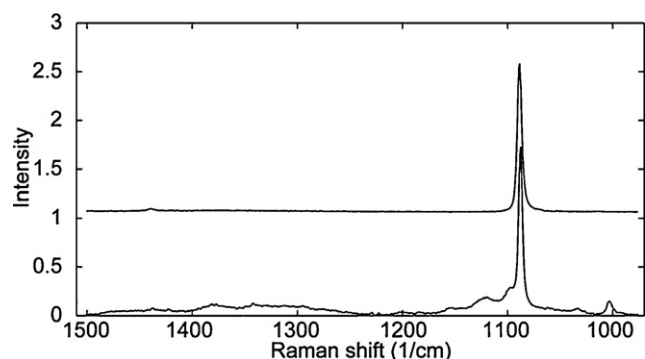


Fig. 5. Raman spectrum of calcium carbonate (top) and counterfeit package box material (inside of box where there is no color) (bottom).

location, in other words, in different regions of the mapped regions, the intensity of this peak varies. There are several cross peaks correlated to the 1087 cm^{-1} peak. A cross peak in a synchronous map shows where two peaks, occurring at different wavenumbers in a one-dimensional spectrum, are changing simultaneously. Cross peaks can be either negative or positive. Positive cross peaks indicate the corresponding peaks are varying in the same direction (both either increasing or decreasing). Negative cross peaks indicate that they are varying in the opposite direction. In the current analysis, positive peaks can be interpreted as peaks that are most likely chemically similar in nature (same material) while negative peaks are chemically dissimilar (different materials). The negative cross peaks at $(1480\text{ cm}^{-1}, 1087\text{ cm}^{-1})$, $(1379\text{ cm}^{-1}, 1087\text{ cm}^{-1})$, $(1293\text{ cm}^{-1}, 1087\text{ cm}^{-1})$, $(1121\text{ cm}^{-1}, 1087\text{ cm}^{-1})$,

and $(1098\text{ cm}^{-1}, 1087\text{ cm}^{-1})$ clearly indicate that the 1480 cm^{-1} , 1379 cm^{-1} , 1293 cm^{-1} , 1121 cm^{-1} , and 1098 cm^{-1} peaks are varying in an opposite way to the 1087 cm^{-1} peak. These peaks (1480 cm^{-1} , 1379 cm^{-1} , 1293 cm^{-1} , 1121 cm^{-1} , and 1098 cm^{-1}) are the characteristic peaks of the box material; the box spectrum was obtained by scanning the inside of the carton which was not printed. The major component of the box material is cellulose; cellulose is one of the most common raw materials in paper production [26] and these peaks can clearly be assigned to cellulose (Fig. 4). The underlying box material can thus be readily observed when the white region of the box is analyzed. There are two positive cross peaks at $(1436\text{ cm}^{-1}, 1087\text{ cm}^{-1})$ and $(1002\text{ cm}^{-1}, 1087\text{ cm}^{-1})$. The 1436 cm^{-1} can also be found in a spectrum of calcium carbonate (Fig. 5) along with the stronger peak at 1087 cm^{-1} . These two peaks belong to the same material, therefore a positive cross peak can be found in the synchronous map. The 1002 cm^{-1} peak can be found in the original spectra, however it cannot be found in the spectrum of calcium carbonate (Fig. 5). This means that there is another material besides calcium carbonate and cellulose in this color region. Although the 1002 cm^{-1} peak does not belong to calcium carbonate, the positive cross peak implies that they are varying in intensity in the same direction. This suggests that these two materials are homogeneously mixed. Therefore, the 1002 cm^{-1} peak is very likely a coating binder used to bind pigments. One of the most common coating binders is styrene butadiene and the most intense peak in the Raman spectrum of this binder occurs at 1002 cm^{-1} [27], this suggests that the package contains styrene butadiene or a styrene-based polymer/copolymer. Thus for the genuine packaging, it appears that calcium carbonate is used to produce the white color, but is not used as a filler in the box material.

The asynchronous spectrum is shown in Fig. 3b. For asynchronous maps, no autopeaks are present and cross peaks can be either positive or negative. In this case, cross peaks only show up along the 1087 cm^{-1} line. Cross peaks are located at $(1095\text{ cm}^{-1}, 1087\text{ cm}^{-1})$, $(1120\text{ cm}^{-1}, 1087\text{ cm}^{-1})$, $(1153\text{ cm}^{-1}, 1087\text{ cm}^{-1})$, $(1340\text{ cm}^{-1}, 1087\text{ cm}^{-1})$, and $(1381\text{ cm}^{-1}, 1087\text{ cm}^{-1})$. Asynchronous peaks appear when the peak intensities are changing out of phase from each other. In this case, the asynchronous peaks most likely account for the different spectral origins of the sample; the box material and the white pigment, calcium carbonate. Most of these peaks can be found from the negative peaks of the synchronous map and essentially can be interpreted the same way. This shows that 2dcos is able to resolve peaks from different spectral origins that are close to one another. Univariate Raman images can be used to confirm these interpretations. For example, the Raman image based on the 1121 cm^{-1} cellulose peak is

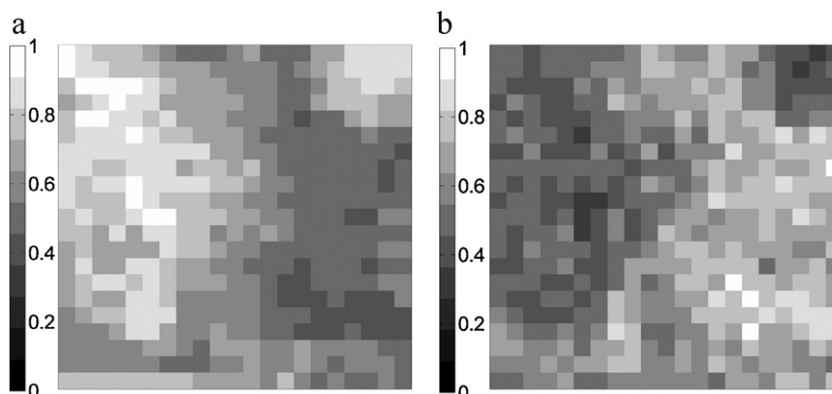


Fig. 6. Raman images of white color region of genuine package (a: variation in intensity of 1087 cm^{-1} peak; b: variation in intensity of 1121 cm^{-1} peak).

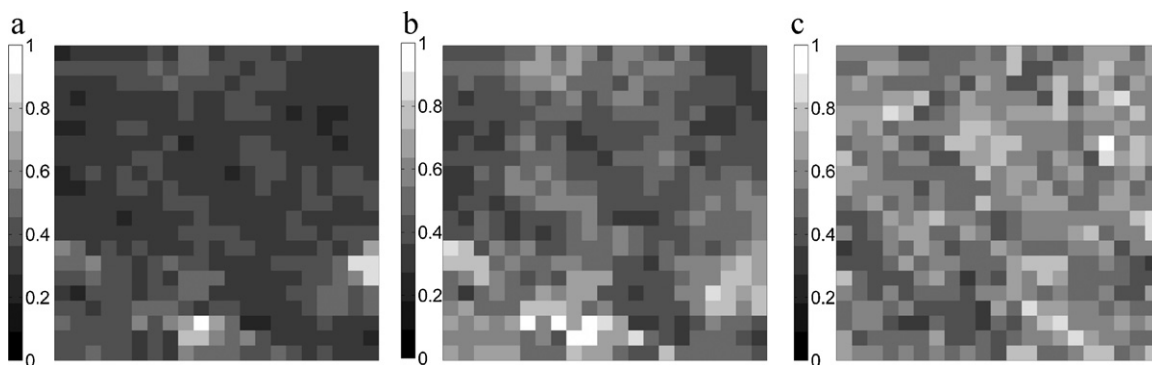


Fig. 7. Raman images of white color region of counterfeit package (a: variation in intensity of 1087 cm^{-1} peak; b: 1097 cm^{-1} peak; c: variation in intensity of 1170 cm^{-1} peak).

approximately the negative of the image based on the calcium carbonate 1087 cm^{-1} peak (Fig. 6). This confirms that the cross peaks in the asynchronous spectrum arise from different origins.

Raman spectra of the counterfeit package in this color region are shown in Fig. 2b. It appears to be more complex than the genuine package spectra. The strongest peak in this set of spectra is located at 1087 cm^{-1} (CaCO_3). This peak is also the strongest peak observed for the genuine package spectra. However, the overall appearance of the spectra is different from the genuine ones with larger variation being observed among the spectra, particularly around the 1100 cm^{-1} region. The synchronous and asynchronous maps are shown in Fig. 3. In contrast to the genuine packaging where only one autopeak at 1087 cm^{-1} was observed, the synchronous map for the counterfeit has two main autopeaks at 1087 cm^{-1} and 1097 cm^{-1} , which implies that there are strong intensity variations in these two peaks. Furthermore, the negative cross peak at $(1087\text{ cm}^{-1}, 1097\text{ cm}^{-1})$ implies that these two peaks are changing in opposite directions. This pair also appears in the asynchronous map which means that these two peaks likely belong to different chemical origins. For this counterfeit sample, the 1087 cm^{-1} peak (CaCO_3) is actually a dominant peak found in the spectrum obtained from the unprinted box material (Fig. 5), suggesting that it is used as a filler in the box material, in contrast to being used as a colorant for the genuine packaging. Because of the dominance of the peak from the CaCO_3 , the 1097 cm^{-1} peak which belongs to cellulose is actually a spectroscopically minor component of the box material (Fig. 4). There are two positive cross peaks at $(1437\text{ cm}^{-1}, 1087\text{ cm}^{-1})$ and $(1002\text{ cm}^{-1}, 1087\text{ cm}^{-1})$; the 1437 cm^{-1} peak belongs to calcium carbonate whereas the 1002 cm^{-1} peak belongs to a styrene related compound and these indicate that the binder is again homogeneously mixed with calcium carbonate (the filler). Negative cross peaks can be seen at $(1380\text{ cm}^{-1}, 1087\text{ cm}^{-1})$ and $(1170\text{ cm}^{-1}, 1097\text{ cm}^{-1})$. The 1380 cm^{-1} and the 1097 cm^{-1} peaks belong to MCC, while the 1170 cm^{-1} peak belongs to an unknown compound which is thought to be another white colorant since this peak does not belong to any of the known components identified thus far (i.e. cellulose, CaCO_3 and a styrene related compound). The asynchronous map consists of mainly peaks along the 1087 cm^{-1} line which further confirms that the white colorant might not contain any calcium carbonate. Some peaks such as $(1097\text{ cm}^{-1}, 1170\text{ cm}^{-1})$ and $(1097\text{ cm}^{-1}, 1331\text{ cm}^{-1})$ along the 1097 cm^{-1} line implies that the 1170 and 1331 cm^{-1} peaks belong to an unknown compound which contributes as the white colorant or another paper additive. The univariate Raman images at 1087 cm^{-1} , 1097 cm^{-1} , and 1170 cm^{-1} (Fig. 7) show that the distributions of the peak intensities using the three peak positions are not the same which means that there are at least three components in this color region. These components are cellulose, calcium carbonate (with a styrene based compound

mixed in) and an unknown compound. The unknown compound in this area has peaks at 1170 , 1331 , and 1461 cm^{-1} .

3.2. Yellow color region

The Raman spectra of the genuine package are shown in Fig. 8a. From the synchronous map (Fig. 9a), there are three autopeaks located at 1598 cm^{-1} , 1400 cm^{-1} , and 1258 cm^{-1} . Positive cross peaks at 1523 cm^{-1} , 1491 cm^{-1} , 1400 cm^{-1} , 1288 cm^{-1} , 1258 cm^{-1} along the 1598 cm^{-1} line indicate that these peaks are increasing or decreasing with the 1598 cm^{-1} peak. None of these peaks belong to cellulose, calcium carbonate or styrene base compound, so they are most likely contributions from the yellow colorant. In contrast, negative peaks at 1452 cm^{-1} , 1437 cm^{-1} , 1371 cm^{-1} , 1305 cm^{-1} , 1277 cm^{-1} , 1199 cm^{-1} , 1155 cm^{-1} along this line are varying opposite to the 1598 cm^{-1} peak. For instance, the 1437 cm^{-1} peak arises from calcium carbonate. Only cross peaks along the 1598 cm^{-1} , 1400 cm^{-1} , and 1258 cm^{-1} lines can be seen on the synchronous map. The asynchronous map (Fig. 9b) consists of peaks along the 1598 cm^{-1} line as well as wavenumbers other than 1400 cm^{-1} and 1258 cm^{-1} . This indicates that this image is made up of at least three components. For example, two cross peaks at 1438 cm^{-1} and

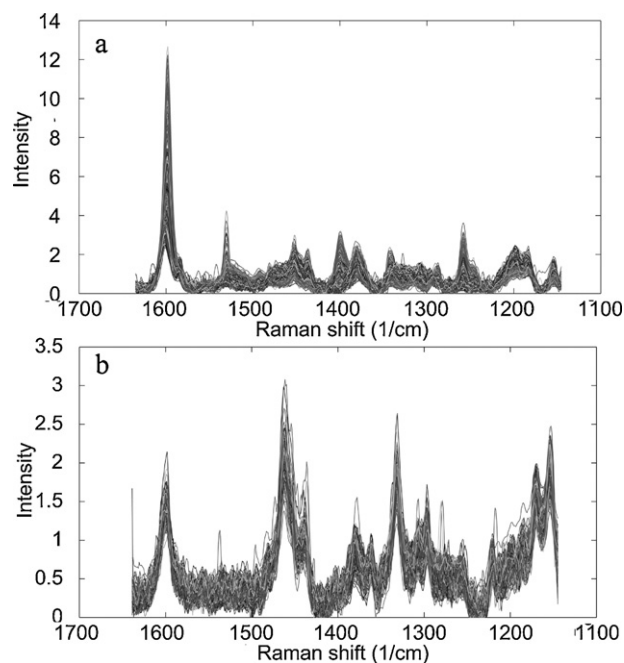


Fig. 8. Raman spectra of the yellow color region (a: genuine; b: counterfeit).

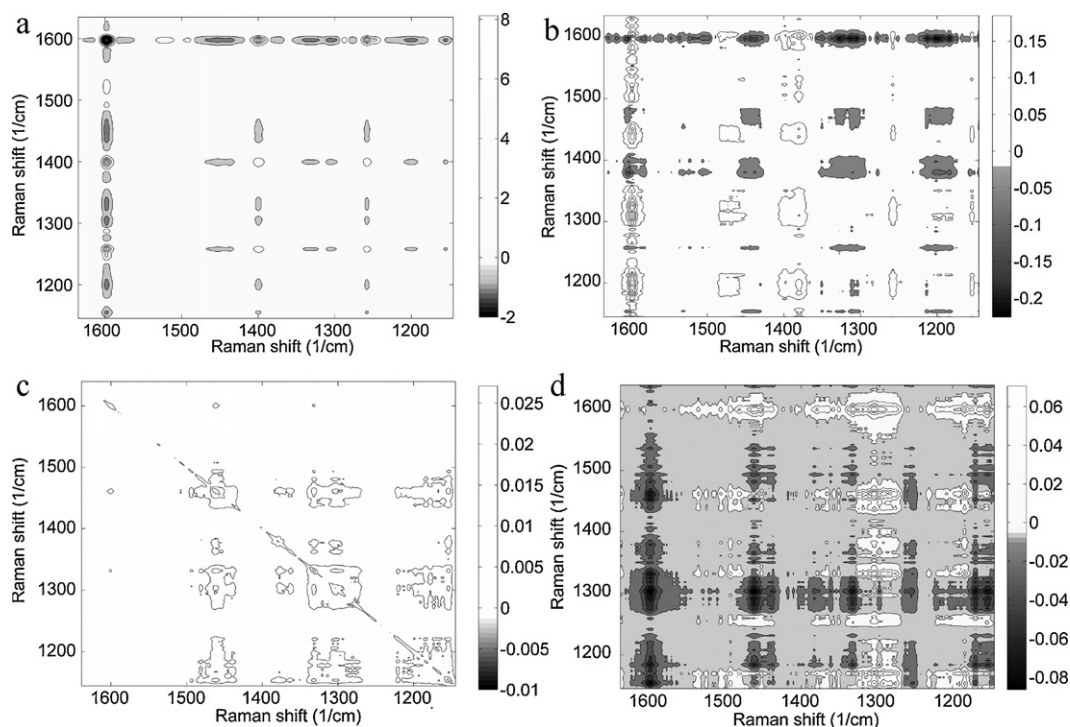


Fig. 9. Synchronous (a and c) and asynchronous (b and d) maps of yellow color region (a and b: genuine; c and d: counterfeit).

1451 cm^{-1} along the 1380 cm^{-1} line showed that these two spectral features are of a different origin from the 1380 cm^{-1} feature which belongs to the box material (cellulose) while the 1438 cm^{-1} and 1451 cm^{-1} come from the white colorant (CaCO_3) and the 1598 cm^{-1} , 1400 cm^{-1} , and 1258 cm^{-1} peaks come from the yellow colorant. In addition to these peaks, the synchronous map indicates that 1491 cm^{-1} and 1288 cm^{-1} peaks also belong to the yellow colorant. Based on the peak profiles, the yellow colorant is most likely an organic compound and a member of the large family of synthetic azo type yellow pigments [28]. A distinct pattern can be seen from the Raman images generated using either the 1599 cm^{-1} or 1452 cm^{-1} peak for monitoring, while the 1380 cm^{-1} peak image showed the pattern of the box material which is rather random (Fig. 10). These images confirm that these three peaks most likely originated from three different chemical components: cellulose, calcium carbonate, and yellow colorant.

The Raman spectra of the counterfeit package in this color region are shown in Fig. 8b. The Raman spectra look quite different from the genuine ones. The strongest peak for the genuine spectra was at 1598 cm^{-1} . There is a peak at 1598 cm^{-1} in the counterfeit spectra,

but it is not the most intense peak as seen in the genuine spectrum and the magnitude of other major peaks are quite similar to each other. The synchronous map in this case does not reveal much correlation among the spectral peaks (Fig. 9c). However, the asynchronous map contains numerous peaks which implies that there is more than one component in this color region. Thus the presence of a peak implies that the pair is dissimilar chemically, such as the 1599 cm^{-1} and the 1331 cm^{-1} peaks. The absence of a peak may imply that the pair is similar such as the 1331 cm^{-1} and the 1154 cm^{-1} peaks which belong to the unknown white colorant or additive. The Raman images (Fig. 11) show that the 1599 cm^{-1} image is different from the images based on the 1331 cm^{-1} and the 1154 cm^{-1} peaks. However, the patterns of the 1331 cm^{-1} and the 1154 cm^{-1} images are somewhat more similar to each other. Furthermore, these images do not show the regular variations in intensity that are seen for the genuine packaging; instead the pixels exhibit random intensity variations at the selected frequencies. This is an indication of a different printing procedure for this counterfeit package. This could also be one of the reasons that no strong correlation can be seen from the synchronous spectrum. The 1599 cm^{-1}

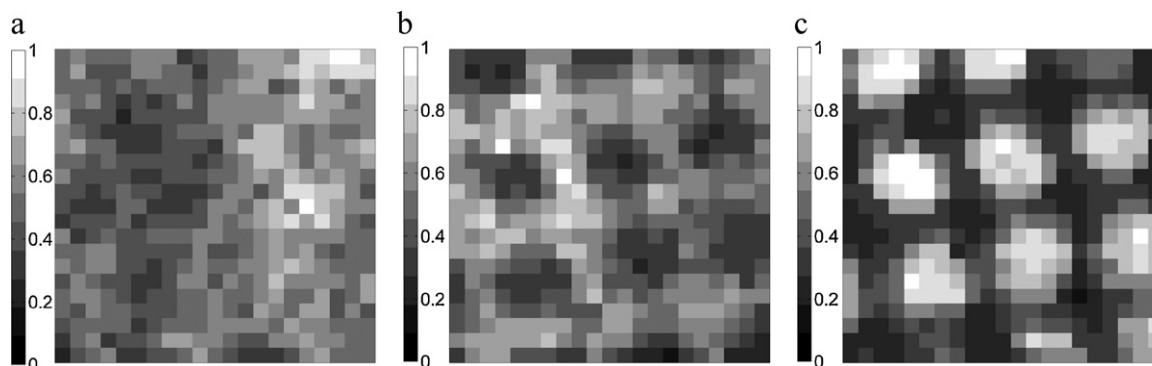


Fig. 10. Raman images of yellow color region of genuine package (a: variation in intensity of 1380 cm^{-1} peak; b: variation in intensity of 1452 cm^{-1} peak; c: variation in intensity of 1599 cm^{-1} peak).

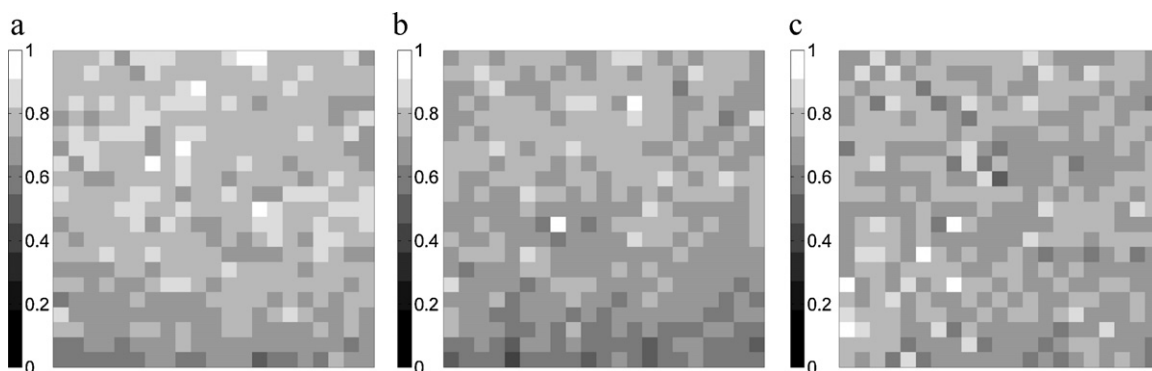


Fig. 11. Raman images of yellow color region of counterfeit package (a: variation in intensity of 1155 cm^{-1} peak; b: variation in intensity of 1331 cm^{-1} peak; c: variation in intensity of 1599 cm^{-1} peak).

peak belongs to the yellow colorant, however it is not clear that this is the same compound as in genuine package since the signal at the other peak positions (e.g. 1400 cm^{-1} , 1258 cm^{-1} , etc.) is too weak to yield any synchronous peaks. Furthermore, the concentration of this yellow colorant seems to be similar to that of the white colorant in this region based on the peak intensities of the original spectra.

Principal component analysis (PCA) is a more popular and common chemometric technique used in the analysis of chemical data. Although PCA can be used to reduce the dimension of the data matrix and determine the number of significant components in the system and the group of variables correspond to each component, 2dcos can be used to determine the in phase and out of phase changes among variables. For instance, the out of phase relations can be used to determine the important sequential relations of a chemical reaction. 2dcos analysis can readily generate a visual map in the spectral space instead of the abstract principal component space which makes it more intuitive to be understood and readily interpreted. Although only two maps (synchronous and asynchronous) can be generated by the 2dcos analysis as opposed to the multiple principal components by PCA, it has been demonstrated in this study that more than two components can be deduced by careful comparison and interpretation of these two maps. Therefore, 2dcos is a valuable and complementary chemometric technique to be used in the analysis of spectroscopic data sets.

4. Conclusions

Raman imaging has been combined with two-dimensional correlation spectroscopy to analyze and compare genuine and counterfeit Cialis[®] packages. Different components from two color regions of the packages can be distinguished by this technique. The white color region of the genuine package was made of cellulose (box), calcium carbonate (white pigment), and a styrene based compound (coating binder), while for the counterfeit package it consisted of cellulose, calcium carbonate (box), a styrene based compound, and an unknown white colorant. For the yellow color region, in addition to the components found in the white color area, both the genuine and the counterfeit packages contain an unknown yellow colorant which may be chemically dissimilar. It has been shown that 2dcos is capable of identifying peaks that belong to the same component within a microscopic area of the package. Univariate Raman images based on peak intensities were used to show the spatial distribution of different components and confirm the 2dcos analyses. This research also showed that the resolving power of 2dcos can be used to estimate or predict the number of components in a multicomponent system before subjecting the data to further chemometric analysis.

Acknowledgments

This work was supported by a grant from the Lilly Endowment Inc. to the College of Pharmacy and a research fellowship from United States Pharmacopeia to K.K.

References

- [1] F.M. Fernandez, M.D. Green, P.N. Newton, *Ind. Eng. Chem. Res.* 47 (2008) 585–590.
- [2] Consumer Updates > Warning: Counterfeit Alli 25 January, 2010, The Food and Drug Administration, 13 June, 2011, <http://www.fda.gov/ForConsumers/ConsumerUpdates/ucm198557.htm>.
- [3] Deadly counterfeit diabetes drug found outside China's Xinjiang, *English_Xinhua* 4 February, 2009, The Xinhua News Agency, 13 June, 2011, http://news.xinhuanet.com/english/2009-02/05/content_10765031.htm.
- [4] Fake batches of Eli Lilly drug Zyprexa found in UK | Reuters 24 May, 2007, Thomson Reuters, 13 June, 2011, <http://uk.reuters.com/article/2007/05/24/uk-lilly-britain-idUKL2446370820070524>.
- [5] WHO, Medicines: counterfeit medicines 7 December, 2010, The World Health Organization, 13 June, 2011, <http://www.who.int/mediacentre/factsheets/fs275/en/index.html>.
- [6] I. Noda, *Appl. Spectrosc.* 47 (1993) 1329–1336.
- [7] I. Noda, A.E. Dowrey, C. Marcott, G.M. Story, *Appl. Spectrosc.* 54 (2000) 236A–248A.
- [8] I. Noda, *Appl. Spectrosc.* 54 (2000) 994–999.
- [9] I. Noda, Y. Ozaki, *Two-Dimensional Correlation Spectroscopy: Applications in Vibrational and Optical Spectroscopy*, 1st ed., John Wiley and Sons, New York, 2004.
- [10] R. Vehring, *Appl. Spectrosc.* 59 (2005) 286–292.
- [11] D. Pratiwi, J.P. Fawcett, K.C. Gordon, T. Rades, *Eur. J. Pharm. Biopharm.* 54 (2002) 337–341.
- [12] J. Rantanen, H. Wikström, F.E. Rhea, L.S. Taylor, *Appl. Spectrosc.* 59 (2005) 942–951.
- [13] H. Wikström, W.J. Carroll, L.S. Taylor, *Pharm. Res.* 25 (2008) 923–935.
- [14] M. Savolainen, K. Jouppila, O. Pajamo, L. Christiansen, C. Strachan, M. Karjalainen, J. Rantanen, *J. Pharm. Pharmacol.* 59 (2007) 161–170.
- [15] M. Savolainen, K. Kogermann, A. Heinz, J. Aaltonen, L. Peltonen, C. Strachan, J. Yliruusi, *Eur. J. Pharm. Biopharm.* 71 (2009) 71–79.
- [16] F.C. Clarke, M.J. Jamieson, D.A. Clark, S.V. Hammond, R.D. Jee, A.C. Moffat, *Anal. Chem.* 73 (2001) 2213–2220.
- [17] T. Kojima, S. Onoue, N. Murase, F. Katoh, T. Mano, Y. Matsuda, *Pharm. Res.* 23 (2006) 806–812.
- [18] H. Shinzawa, K. Awab, T. Okumura, S. Morita, M. Otsuka, Y. Ozaki, H. Sato, *Vib. Spectrosc.* 51 (2009) 125–131.
- [19] H.G.M. Edwards, D.W. Farwell, F.R. Perez, S.J. Villar, *J. Raman Spectrosc.* 30 (1999) 307–311.
- [20] T.D. Chaplin, R.J.H. Clark, D.R. Beech, *J. Raman Spectrosc.* 33 (2002) 424–428.
- [21] K.L. Brown, R.J.H. Clark, *Anal. Chem.* 74 (2002) 3658–3661.
- [22] A.M. Correia, R.J.H. Clark, M.I.M. Ribeiro, M.L.T.S. Duarte, *J. Raman Spectrosc.* 38 (2007) 1390–1405.
- [23] B. Cappel, I.M. Bell, L.K. Pickard, *Appl. Spectrosc.* 64 (2010) 195–200.
- [24] C.A. Lieber, A. Mahadevan-Jansen, *Appl. Spectrosc.* 57 (2003) 1363–1367.
- [25] A. Savitzky, M.J.E. Golay, *Anal. Chem.* 36 (1964) 1627–1639.
- [26] S. Bell, *Forensic Chemistry*, 1st ed., Pearson Education, New Jersey, 2006.
- [27] P. He, S. Bitla, D. Bousfield, C.P. Tripp, *Appl. Spectrosc.* 56 (2002) 1115–1121.
- [28] P. Ropret, S.A. Centeno, P. Bukovec, *Spectrochim. Acta Part A* 69 (2008) 486–497.